PHYSICAL REVIEW B **78**, 024409 (2008)

Strong linewidth variation for spin-torque nano-oscillators as a function of in-plane magnetic field angle

K. V. Thadani,[1] G. Finocchio,[2] Z.-P. Li,[1] O. Ozatay,[1] J. C. Sankey,[1] I. N. Krivorotov,[3] Y.-T. Cui,[1] R. A. Buhrman,[1] and D. C. Ralph[1]

[1]*Cornell University, Ithaca, New York 14853, USA*

[2]*Dipartimento di Fisica della Materia e Tecnologie Fisiche Avanzate, University of Messina, Salita Sperone 31, 98166 Messina, Italy*

[3]*Department of Physics and Astronomy, University of California, Irvine, California 92697, USA*

(Received 2 June 2008; published 14 July 2008)

We measure the microwave signals produced by spin-torque-driven magnetization dynamics excited by direct currents in patterned magnetic multilayer devices at room temperature as a function of the angle of a magnetic field applied in the sample plane. We find strong variations in the frequency linewidth of the signals, with a decrease by more than a factor of 20 as the field is rotated from the magnetic easy axis to the in-plane hard axis. Based on micromagnetic simulations, we identify these variations as due to a transition from spatially incoherent to coherent precession.

DOI: 10.1103/PhysRevB.78.024409 PACS number(s): 75.75.+a, 72.25.−b, 76.50.+g

I. INTRODUCTION

In a magnetic multilayer device, spin-transfer torque from a spin-polarized direct current (DC) can excite steady-state magnetic precession,[1,2] thereby creating a nanoscale frequency-tunable microwave source.[3–17] Such nano-oscillators have been studied previously in two device geometries: nanopillars in which the precession occurs in a finite disk of magnetic material[3,5,6,8,9,12–14,16,17] and point-contact devices in which precession is excited within a small region that is part of a larger-area magnetic thin film.[4,7,10,11,15] For applications, it is desirable that the microwave signal has a frequency spectrum with a narrow linewidth at room temperature. For this reason, understanding what physical processes affect the linewidth has generated considerable interest, both theoretically[18–22] and in experiments that have explored the dependence on temperature[12,13] and on magnetic fields which rotate the precession axis out of the sample plane.[5–7,9,15] It is important to note that the mechanisms governing the linewidth of DC-driven precession differ from the physics of the linewidth in ferromagnetic resonance (FMR) experiments excited by oscillatory drives,[12] and, in fact, these two different types of linewidth can differ by more than a factor of 10 in the same sample.[23] The FMR linewidth is determined directly by the magnetic damping parameter, while the linewidth of DC-driven precession is determined by deviations from perfect periodicity in the precessional trajectories. Here we report measurements and simulations of DC-driven precession which show a surprisingly strong dependence of this linewidth on the in-plane angle of applied magnetic field. We find that the most-commonly studied field orientation, in-plane and parallel to the magnetic easy axis, produces the broadest linewidths. As the field angle is rotated toward the in-plane hard axis the linewidths decrease dramatically, by more than a factor of 20 in some devices. Comparisons with micromagnetic simulations suggest that this change is due to a crossover from spatially incoherent to coherent dynamics.

II. DEVICE FABRICATION AND CHARACTERIZATION

We will report results from two types of multilayer devices, both with a nanopillar geometry. In both cases the magnetic "free layer" that precesses has 4 nm of Permalloy (Py, $Ni_{81}Fe_{19}$). In the first geometry, the magnetic "fixed layer" that polarizes the current is 4 nm of Py exchange-biased to a layer of antiferromagnetic IrMn. The full layer structure is (with thicknesses in nanometers) 4 Py/80 Cu/8 IrMn/4 Py/8 Cu/4 Py/20 Cu/30 Pt and a Cu top contact. The second type of sample has a thicker Py fixed layer (20 nm) with no exchange bias: 2 Py/120 Cu/20 Py/12 Cu/4 Py/12 Cu/30 Pt with a Cu top contact. The samples are fabricated using the procedure described in Ref. 24. First the layers are deposited by sputtering, and then electron-beam lithography and ion milling are used to etch through both the free and fixed magnetic layers to the bottom Cu contact, giving a device cross section that is approximately elliptical [Fig. 1(a), inset]. The minor diameter of the cross section is 50–70 nm, and we have studied samples with aspect ratios of both 2:1 and 3:1. We use photolithography to pattern bottom leads and to make top contacts. For the exchange-biased samples, we sputter the layers in a magnetic field (300 Oe) and anneal at 220 °C for 85 min before patterning to pin the fixed-layer direction along the long axis of the ellipse. In this paper, we will show data from one 50×150 nm^2 exchange-biased fixed-layer device (with the exchange bias directed along the long axis of the ellipse) and one 70×130 nm^2 thick-fixed-layer device. Similar results were obtained in 17 exchange-biased samples and 5 thick-fixed-layer samples.

Figure 1 shows the differential resistance (dV/dI) as a function of current (I) and magnetic field (H) for the two devices at room temperature. The behavior is very similar to that of devices reported previously.[3] For the device with the exchange-biased fixed layer, as the current is swept [Fig. 1(a)], at low magnetic fields we observe hysteretic switching between the parallel and antiparallel magnetic orientations with a resistance change at zero bias $\Delta R=0.094\ \Omega$, and above $H=450$ Oe we find nonhysteretic peaks in dV/dI that are associated with transitions among precessional and static

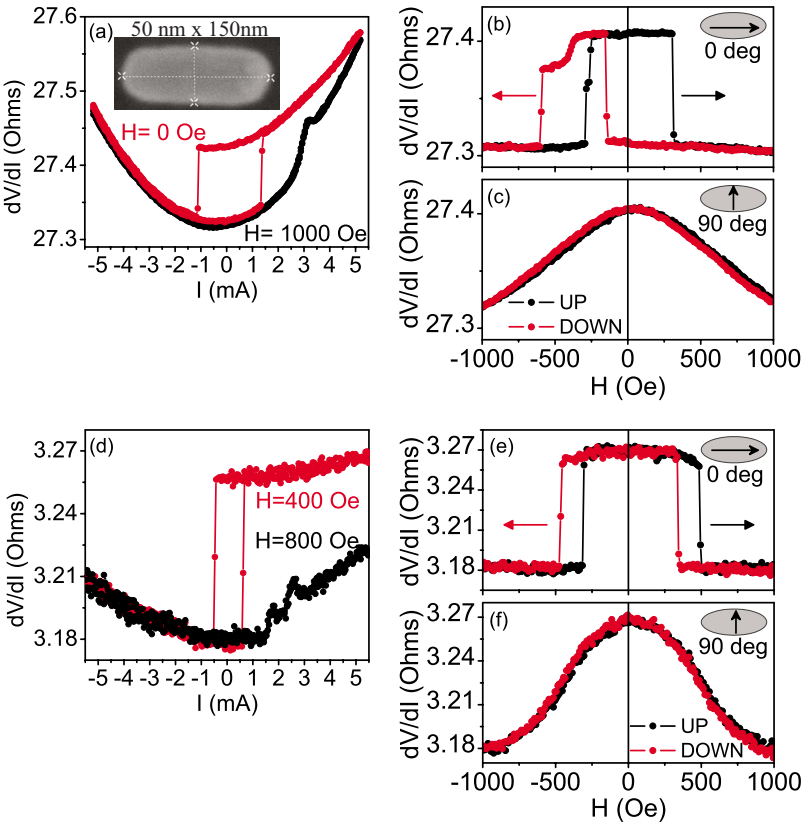

FIG. 1. (Color online) (a) Differential resistance as a function of current at room temperature for a nanopillar spin valve device with an exchange-biased fixed layer. Inset: top-view electron micrograph of device shape. [(b) and (c)] Resistance as a function of magnetic field for the same device for fields (b) along the easy-axis direction and (c) along the in-plane hard axis. [(d)–(f)] Differential resistance of a nanopillar spin valve device with a thick-fixed layer as a function of (d) current and [(e) and (f)] magnetic field at room temperature.

magnetic states. At zero bias, as the magnetic field is swept in the direction of the long axis of the sample cross section (the magnetic easy axis, "0°") [Fig. 1(b)], we observe switching of the magnetic layers between parallel and antiparallel alignments. The transitions on the right in Fig. 1(b) are associated with transitions of the magnetic free layer. From these, we infer that the effective dipole field of the fixed layer acting on the free layer is $H_{\mathrm{dipole}}=80$ Oe and the coercive field of the free layer at room temperature is $H_{\mathrm{an}} \approx 200$ Oe. From the transitions on the left, we find that the sum of the exchange bias and effective field on the fixed layer is $H_{\mathrm{eb}}=360$ Oe. As the field is swept in the perpendicular in-plane direction (the in-plane hard axis, "90°") [Fig. 1(c)], the angle between the layers changes smoothly from the antiparallel orientation to parallel. The device with the thick fixed layer [Figs. 1(d)–1(f)] is similar, except that the 0° magnetic-field sweep shows no exchange bias acting on the fixed layer. For this device, from minor loops for the free layer, we determine $H_{\mathrm{dipole}}=400$ Oe and $H_{\mathrm{an}} \approx 100$ Oe.

III. EXPERIMENTAL DATA AND ANALYSIS

Our main focus in this paper will be high-frequency voltage oscillations produced by spin-torque-driven magnetic precession driven by a direct current. These oscillations arise because precession of the magnetic moment of the free layer causes microwave-frequency changes in the resistance of the magnetic multilayer due to the giant magnetoresistance (GMR) effect, and in the presence of a DC bias these produce voltage oscillations according to Ohm's law. We measure the frequency spectrum of the voltage oscillations using a heterodyne mixer circuit. We perform all measurements at room temperature, with a large in-plane magnetic field applied using a projected field electromagnet[25] that allows us to control the field angle θ_H continuously. For the field values used in our experiment (800–1000 Oe), both the measured resistances and macrospin modeling using the parameters determined above indicate that for the exchange-biased samples the offset angle between the magnetic moments of the two layers grows from 0° to ~35° as θ_H is increased from 0° to 90°, while for the thick-fixed-layer devices without exchange bias the offset angle is always $<5°$.

Figures 2(a) and 2(b) show DC-driven spectra for the exchange-biased device at 1000 Oe and the thick-fixed-layer device at 800 Oe at selected values of θ_H. The current bias is 5 mA, significantly larger than the critical current needed to excite magnetization dynamics for any θ_H. In the exchange-biased device, when H is applied along the magnetic easy axis in the direction of the exchange bias ($\theta_H=0°$), there is no visible precessional peak, just a low-frequency tail indicating aperiodic dynamics. A precessional peak is first resolvable for $\theta_H \approx 25°$, and at $\theta_H=45°$ there is a broad peak near 6 GHz with a linewidth [full width at half maximum (FWHM)] of 2 GHz, along with a smaller second-harmonic

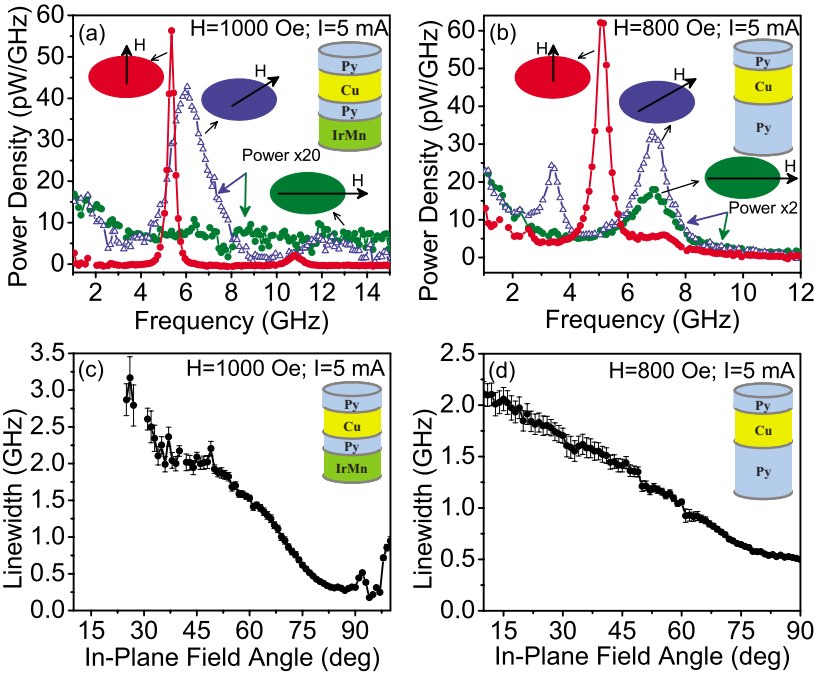

FIG. 2. (Color online) Power spectral density of spin-torque-driven oscillations at room temperature, for field angles θ_H=0°, 45°, and 90° (as labeled), for (a) an exchange-biased-fixed-layer sample and (b) a thick-fixed-layer sample. Insets: sample structures. [(c) and (d)] Variation of the linewidth as a function of θ_H for both types of samples.

peak. As θ_H is increased further toward 90°, the linewidth decreases dramatically. The minimum linewidth for I =5 mA is 170 MHz at θ_H=95°, a factor of 20 narrower than at $\theta_H \approx 25°$ [Fig. 2(c)]. If one selects the current and field magnitudes at which the linewidth narrowing is largest, we observe narrowings as a function of θ_H ranging from a factor of 10 to 50 in all of our exchange-biased samples. We do not show in this paper the devices in which the factor of 50 was observed because the narrowest peaks were limited by the resolution bandwidth chosen for the measurements.

We see a similar but somewhat less dramatic dependence of linewidth on θ_H for the thick-fixed-layer device [Figs. 2(b) and 2(d)]. In this case a broad precessional peak is visible even for θ_H=0° at a frequency corresponding to the second harmonic of the precessional frequency. At θ_H=45°, this second-harmonic peak has narrowed by about 30% and a peak at the fundamental precession frequency is also visible. For θ_H=90°, the second-harmonic frequency is again much larger than the fundamental, and the linewidth of the second harmonic reaches a minimum of 450 MHz, a factor of 5 less than the linewidth at θ_H=0°. We observed linewidth narrowing as a function of θ_H by factors between 2 and 5 in all of our thick-fixed-layer devices.

For the analysis in this paper, we will focus on the linewidth of the spectral peak at the fundamental precessional frequency for the exchange-biased fixed-layer sample and the second harmonic of the thick-fixed-layer sample because these are the largest signals. The reason that the fundamental peak and the second-harmonic peak have different relative amplitudes in the two samples can be understood from the magnitude of the offset angle between the fixed and free layer magnetic moments at I=0. For the range of magnetic field strengths that we apply, there is a nonzero offset angle between the magnetic moments in the exchange-biased fixed-layer sample whenever $\theta_H \neq 0°$ or 180°. Due to the nonzero offset angle, small-angle magnetic precession of the free layer produces a time-varying resistance signal with a fundamental frequency equal to the precession frequency. For the case of the thick-fixed-layer sample, the absence of an exchange-bias layer causes the offset angle between the fixed and free layer magnetizations to be much smaller and to go to zero for θ_H=0° and 90°, where the moments of both magnetic layers should be saturated along the field direction. When the precession amplitude is larger than the equilibrium offset angle, one cycle of precession produces two cycles of resistance, so the dominant signal should be at the second harmonic of the precession frequency. It is a coincidence that the first-harmonic signal in Fig. 2(a) and the second harmonic in Fig. 2(b) both occur near the same frequency when θ_H=90°. This is the result of the large value of H_{dipole} in the thick-fixed-layer sample, which points opposite to the external field acting on the free layer, so that it reduces the total field and therefore also reduces the precessional frequency of the free layer, compared to the exchange-biased fixed-layer sample.

In order to determine why the linewidths vary so strongly, we have analyzed the linewidth, precession frequency, and power of the precessional signals as a function of field angle and current for the two types of samples. For the exchange-biased-fixed-layer sample (Fig. 3), as a function of increasing field angle up to $\theta_H \approx 90°$ the signal displays a decreasing frequency and an increasing total power, together with the decreasing linewidth. The increasing power suggests that the precession amplitude grows as a function of θ_H at fixed current, while the frequency shift is consistent with an increasing demagnetization field and an increased precession ampli-

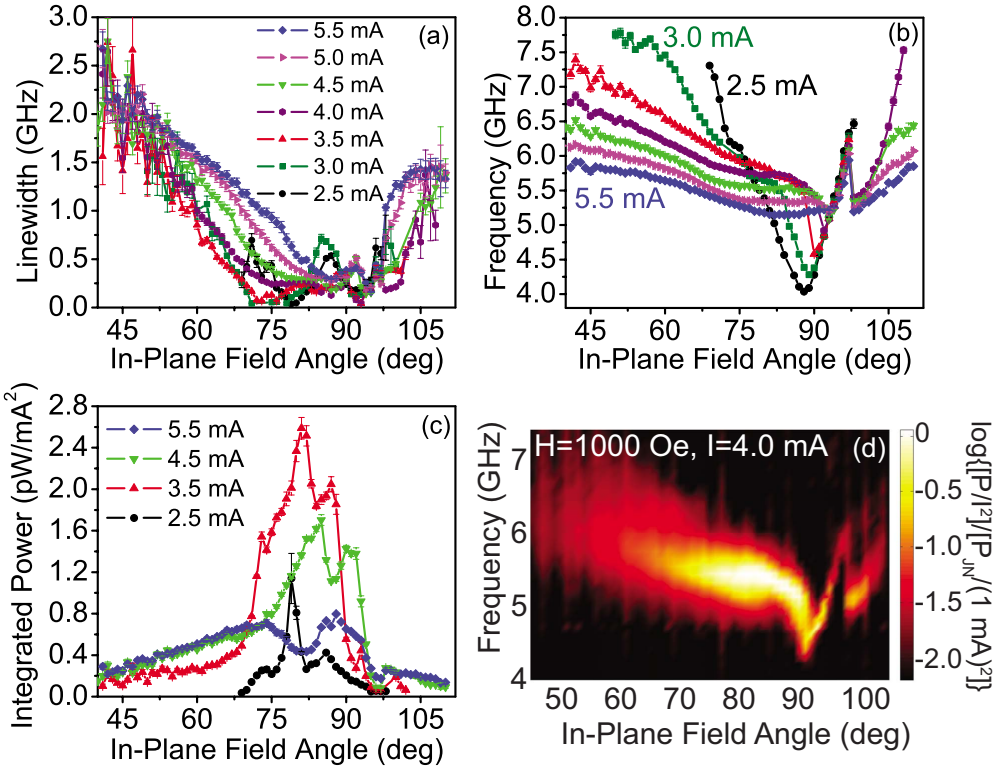

FIG. 3. (Color online) Analysis of the spin-torque-driven microwave signals for the sample with the exchange-biased fixed layer as a function of current and field angle at room temperature and $H=1000$ Oe. (a) Linewidth. (b) Peak frequency. (c) Integrated power within the precessional peak divided by I^2. (d) Power spectral density plotted on a logarithmic scale, as a function of θ_H, for $I=4$ mA.

tude. The narrowest linewidths are observed for θ_H between 75° and 95°, and for small currents (2.5–4 mA), the minimum linewidths approach 40 MHz, close to the resolution bandwidth employed in the measurements. Beyond $\theta_H \approx 95°$ (the exact value is current dependent), the total power in the precessional signal drops abruptly by a factor of 10 and the frequency undergoes changes in slope and jumps as a function of θ_H. We suspect that these changes may be associated with transitions in the magnetization state of the fixed layer. The dependence of the power spectrum on θ_H (for $I=4$ mA) is summarized in a logarithmic-scale plot in Fig. 3(d). We note that the lack of symmetry about $\theta_H=90°$ in all of the panels of Fig. 3 shows that the exchange bias of the fixed layer is still playing a role, even though the magnitude of the applied magnetic field is greater than the exchange-bias field. The dynamics show no dependence on whether θ_H is swept up (0°–180°) or down (180°–0°).

For the thick-fixed-layer sample (Fig. 4), the linewidths generally decrease with θ_H between $\theta_H=0°$ and 90° and increase between $\theta_H=90°$ and 180° at all currents. In the ranges 30°–75° and 105°–130° the fits appear to suggest a nonmonotonic dependence on θ_H, with peaks and abrupt jumps, but these are likely just artifacts of the fitting procedure, associated with the fact that the spectra at these angles seem to consist of two closely spaced peaks [see Fig. 4(d)] that are not well described by Lorentzian fits. The measured frequencies vary smoothly as a function of θ_H [Fig. 4(b)], with a form that is approximately symmetric about $\theta_H=90°$, as expected in the absence of any exchange bias. As noted already in Fig. 2, the decrease in the linewidth between $\theta_H=0°$ and 90° for the thick-fixed-layer sample is less dramatic than the factor of 10–50 observed for the exchange-biased fixed-layer samples.

Since the free magnetic layer is nominally identical in the two kinds of samples (4 nm of Py), based on the large difference in the magnitude by which the linewidths narrow as well as the differences in symmetry about $\theta_H=90°$ in the two kinds of samples, we suggest that the orientation of the fixed layer must play an important role in the degree of coherence of the free layer. We have confirmed that the mode which is excited at different θ_H is always a free layer mode in both types of samples. This was determined by conducting spin-transfer-driven ferromagnetic resonance (ST-FMR) measurements[26,23] on the samples as a function of θ_H; the sign of the ST-FMR signals corresponds to a free layer mode and not the lowest-frequency fixed-layer mode.[23]

IV. SIMULATIONS AND DISCUSSION

We have performed both simple macrospin modeling and more detailed micromagnetic calculations in an attempt to understand these results. In the macrospin simulations, we explored a range of parameters chosen to approximate the sample characteristics and found some narrowing in the predicted linewidths as θ_H is increased from 0° to 90° at room temperature, but only by a factor of 2–3, not by the much larger factor observed experimentally. The macrospin simulations also predict that steady-state precession is stable over a much narrower range of current than we find experimentally. Tiberkevich and Slavin[27] reported that they are able to

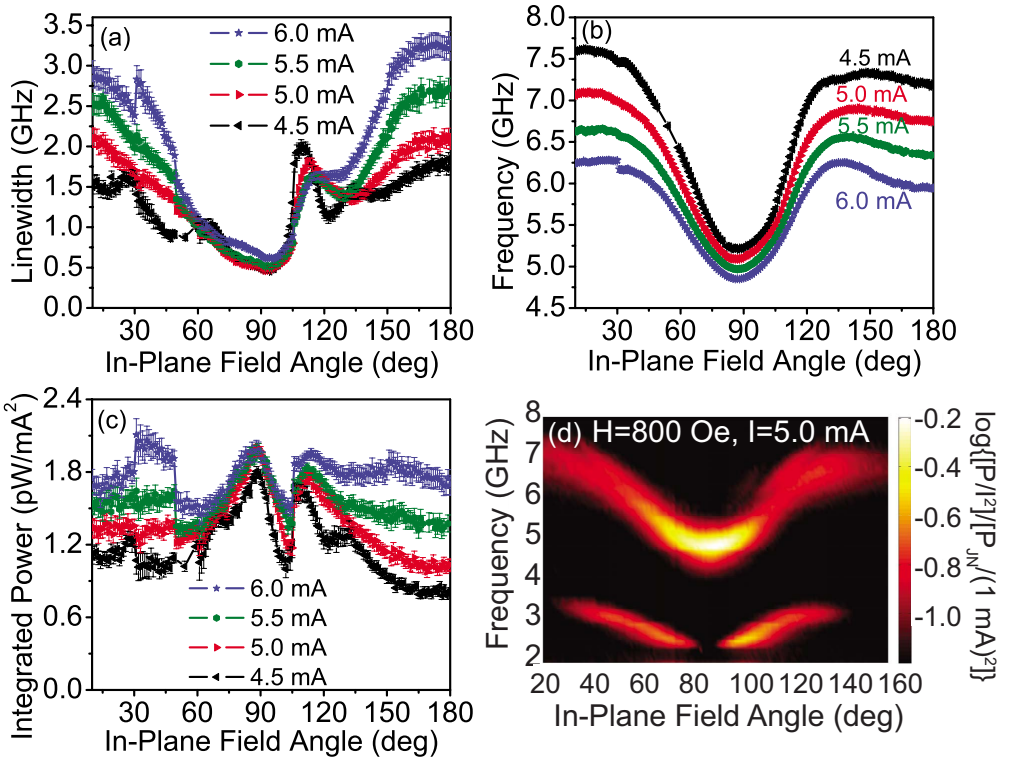

FIG. 4. (Color online) Analysis of the spin-torque-driven microwave signals for the sample with the thick-fixed layer at room temperature and $H=800$ Oe. (a) Linewidth. (b) Peak frequency. (c) Integrated power divided by I^2. (d) Power spectral density plotted on a logarithmic scale, as a function of θ_H, for $I=5$ mA.

fit the large changes in linewidth that we observe using a stochastic nonlinear oscillator equation for the dominant spin-wave mode. However, their calculations do not seem to agree with our macrospin simulations, which we believe should be equivalent. We are puzzled by this difference.

Whereas our macrospin simulations are unable to explain the large linewidth changes we measure, micromagnetic calculations give better agreement. We performed simulations using the algorithms described in Ref. 28, which integrate the Landau-Lifshitz-Gilbert equation for both magnetic layers and include a Slonczewski spin-torque term,[29] the Oersted field from the current, the magnetic interaction between the layers, and fluctuating Langevin fields to model thermal fluctuations. The parameters used in the micromagnetic simulations for the exchange-biased sample are $H=1000$ Oe, $H_{eb}=360$ Oe oriented 20° relative to the easy axis, free and fixed-layer saturation magnetizations $M_S=650$ emu/cm^3, free layer damping $\alpha=0.025$, fixed-layer damping=0.2, temperature=300 K, exchange constant=1.3×10^{-6} erg/cm, GMR asymmetry parameter=1.5, current polarization=0.38, and computational cell size=$5\times5\times4$ nm^3. Each simulation spans 100 ns with a time step of 0.334 ps.

Figure 5(a) shows examples of the simulated resistance as a function of time for an exchange-biased sample. The corresponding spectral densities of the resistance oscillations are shown in Fig. 5(b). We find that, due to thermal fluctuations at room temperature, there is no well-defined precessional peak in the simulated signal between $\theta_H=0°$ and approximately 30°, consistent with our measurements. At $\theta_H=30°$, we see only a broad second-harmonic peak in the simulated spectrum but no first harmonic because of the relatively small misalignment angle between the layers. The first harmonic appears in the simulation at $\theta_H=45°$, and it has a linewidth of about 3.1 GHz. As θ_H is increased to 90°, the linewidth of the first harmonic decreases strongly, eventually reaching a minimum (FWHM) of 350 MHz [Fig. 5(c)]. The minimum linewidth in the simulation is about twice as large as the minimum linewidth of 170 MHz observed at $\theta_H=90°$ in the experiment for the same parameters [Fig. 2(a)]. The simulation predicts a factor of about 10 by which the linewidth narrows between the field angle at which a first-harmonic peak becomes first resolvable in the simulation (i.e., at $\theta_H=45°$) and $\theta_H=90°$. This is close to the factor by which this peak narrows between $\theta_H=45°$ and 90° in the experiment but smaller than the factor of 20 by which it narrows between $\theta_H=25°$ (the field angle at which the peak first becomes resolvable in the experiment) and $\theta_H=90°$.

Similar simulations (not shown) for the thick-fixed-layer sample predict that the linewidth decreases from about 2.5 GHz at $\theta_H=0°$ to about 530 MHz at $\theta_H=90°$. The minimum linewidth in the simulation is quite close to the minimum linewidth of 450 MHz observed at $\theta_H=90°$ in the experiment, and the factor of 5 by which the linewidth narrows is also close to the experimental value.

For both kinds of samples, the micromagnetic simulations suggest that the nature of the magnetization dynamics is qualitatively different for θ_H near 0° and 90°. In Figs. 5(d) and 5(e), we show snapshots of the spatial distribution of the magnetization in the free layer at $T=300$ K for both field

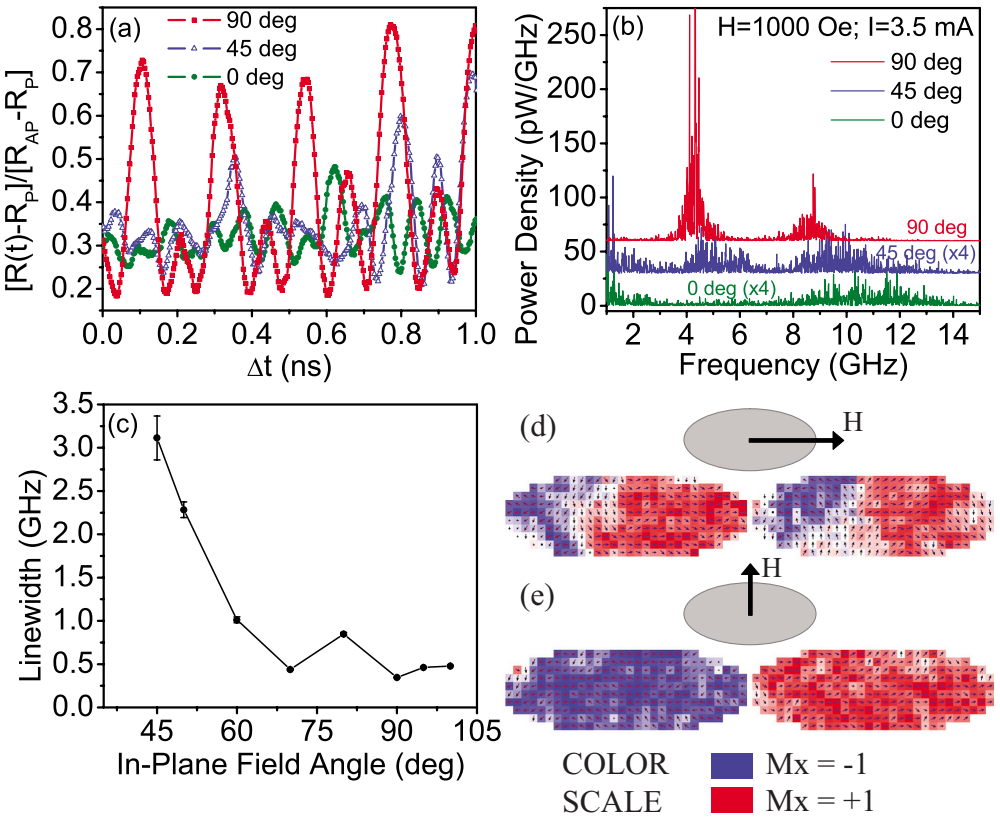

FIG. 5. (Color online) Micromagnetic simulations of the exchange-biased sample. (a) Resistance as a function of time. R_P is the resistance for parallel free and fixed magnetic layers and R_{AP} corresponds to antiparallel layers. (b) Corresponding power spectral densities. The curves for θ_H=45° and 90° are offset by 30 and 60 pW/GHz. The curves for θ_H=0° and 45° are scaled by a factor of 4. (c) Calculated linewidth as a function of θ_H for H=1000 Oe and I=3.5 mA. [(d) and (e)] Snapshots of the magnetization distribution in the magnetic free layer for (d) θ_H=0° and (e) θ_H=90° at times corresponding to maxima in the precession cycle.

angles. The arrows in these plots represent the magnetization in the sample plane and the colors represent the magnetization component parallel to the long axis of the ellipse. For the case of θ_H=0° [Fig. 5(d)], the oscillations are spatially nonuniform and irregular, and the left and right halves of the ellipse can precess in opposite directions. Because different parts of the sample are not precessing together, this spatial incoherence produces temporal incoherence in the resistance signal, broadening the linewidth. In contrast, for the case of θ_H=90° [Fig. 5(e)], the dynamics are nearly spatially uniform, with the whole free layer precessing together in a spatially and temporally coherent manner, to give a precessional trajectory with a very well-defined frequency and a narrow linewidth. For angles near θ_H=45° the magnetization undergoes nanosecond-scale jumps between spatially nonuniform states and the state which is more spatially coherent.

Based on the micromagnetic simulations, we can consider the possible mechanisms underlying the crossover from spatially incoherent to coherent dynamics. One factor may be that the misalignment angle (θ_{mis}) between the fixed and free layer moments grows as θ_H is increased in the exchange-biased samples. When θ_{mis} is much larger than the range of angular variations within the micromagnetic configuration of the free layer, the spin torque on each spatial element will be in the same direction, and this may promote spatially coherent motion.[28] Another important factor may be the amplitude of the precession. In Fig. 5(a), we see that the amplitude of the oscillations is much smaller at θ_H=0° and θ_H=45° than at θ_H=90°. Smaller oscillation amplitudes make the dynamics more sensitive to thermal fluctuations in both amplitude and frequency.[12] A potential mechanism that does not appear to contribute to the crossover between spatially coherent and incoherent dynamics is the Oersted field from the applied current. We performed simulations with the Oersted field both included and absent and found no significant qualitative differences in the dynamics.

V. CONCLUSIONS

In summary, we observe that applying a magnetic field along the hard in-plane axis of a magnetic nanopillar device, so as to offset the precession axis of the free layer away from the orientation of the fixed layer, can produce a dramatic reduction in the linewidth of the spin-torque-driven dynamics excited by a direct current. Based on micromagnetic simulations, we associate this reduction with a crossover from spatially nonuniform magnetization dynamics to spatially coherent precession. This ability to control the spatial uniformity of the magnetization dynamics should help in the development of spin-torque nano-oscillators for use as microwave sources. Our results also suggest that large device-to-device variations in linewidths measured previously[3,8,9,12] may be associated with variations in the angle of the exchange bias relative to the field direction.

ACKNOWLEDGMENTS

We thank B. Azzerboni, L. Torres, P. M. Braganca, C. Wang, and P. G. Gowtham for helpful discussions. We acknowledge support from the NSF/NSEC program through the Cornell Center for Nanoscale Systems, the Office of Naval Research, DARPA, and New York State. We also acknowledge NSF support through use of the Cornell Nanofabrication Facility/NNIN and the Cornell Center for Materials Research facilities.

[1] J. C. Slonczewski, J. Magn. Magn. Mater. **159**, L1 (1996).
[2] L. Berger, Phys. Rev. B **54**, 9353 (1996).
[3] S. I. Kiselev, J. C. Sankey, I. N. Krivorotov, N. C. Emley, R. J. Schoelkopf, R. A. Buhrman, and D. C. Ralph, Nature (London) **425**, 380 (2003).
[4] W. H. Rippard, M. R. Pufall, S. Kaka, S. E. Russek, and T. J. Silva, Phys. Rev. Lett. **92**, 027201 (2004).
[5] M. Covington, M. AlHajDarwish, Y. Ding, N. J. Gokemeijer, and M. A. Seigler, Phys. Rev. B **69**, 184406 (2004).
[6] S. I. Kiselev, J. C. Sankey, I. N. Krivorotov, N. C. Emley, M. Rinkoski, C. Perez, R. A. Buhrman, and D. C. Ralph, Phys. Rev. Lett. **93**, 036601 (2004).
[7] W. H. Rippard, M. R. Pufall, S. Kaka, T. J. Silva, and S. E. Russek, Phys. Rev. B **70**, 100406(R) (2004).
[8] I. N. Krivorotov, N. C. Emley, J. C. Sankey, S. I. Kiselev, D. C. Ralph, and R. A. Buhrman, Science **307**, 228 (2005).
[9] S. I. Kiselev, J. C. Sankey, I. N. Krivorotov, N. C. Emley, A. G. F. Garcia, R. A. Buhrman, and D. C. Ralph, Phys. Rev. B **72**, 064430 (2005).
[10] S. Kaka, M. R. Pufall, W. H. Rippard, T. J. Silva, S. E. Russek, and J. A. Katine, Nature (London) **437**, 389 (2005).
[11] F. B. Mancoff, R. D. Rizzo, B. N. Engel, and S. Tehrani, Nature (London) **437**, 393 (2005).
[12] J. C. Sankey, I. N. Krivorotov, S. I. Kiselev, P. M. Braganca, N. C. Emley, R. A. Buhrman, and D. C. Ralph, Phys. Rev. B **72**, 224427 (2005).
[13] A. V. Nazarov, H. M. Olson, H. Cho, K. Nikolaev, Z. Gao, S. Stokes, and B. B. Pant, Appl. Phys. Lett. **88**, 162504 (2006).
[14] Q. Mistral, J.-V. Kim, T. Devolder, P. Crozat, C. Chappert, J. A. Katine, M. J. Carey, and K. Ito, Appl. Phys. Lett. **88**, 192507 (2006).
[15] W. H. Rippard, M. R. Pufall, and S. E. Russek, Phys. Rev. B **74**, 224409 (2006)
[16] D. Houssameddine, U. Ebels, B. Delaet, B. Rodmacq, I. Firastrau, F. Ponthenier, M. Brunet, C. Thirion, J.-P. Michel, L. Prejbeanu-Buda, M. C. Cyrille, O. Redon, and B. Dieny, Nat. Mater. **6**, 447 (2007).
[17] V. S. Pribiag, I. N. Krivorotov, G. D. Fuchs, P. M. Braganca, O. Ozatay, J. C. Sankey, D. C. Ralph, and R. A. Buhrman, Nat. Phys. **3**, 498 (2007).
[18] S. E. Russek, S. Kaka, W. H. Rippard, M. R. Pufall, and T. J. Silva, Phys. Rev. B **71**, 104425 (2005).
[19] J. V. Kim, Phys. Rev. B **73**, 174412 (2006).
[20] J. V. Kim, V. Tiberkevich, and A. N. Slavin, Phys. Rev. Lett. **100**, 017207 (2008).
[21] C. Serpico, G. Bertotti, R. Bonin, M. d-Aquino, and I. D. Mayergoyz, J. Appl. Phys. **101**, 09A507 (2007).
[22] K. Mizushima, K. Kudo, and R. Sato, J. Appl. Phys. **101**, 113903 (2007).
[23] J. C. Sankey, P. M. Braganca, A. G. F. Garcia, I. N. Krivorotov, R. A. Buhrman, and D. C. Ralph, Phys. Rev. Lett. **96**, 227601 (2006).
[24] N. C. Emley, Ph.D. thesis, Cornell University, 2005.
[25] http://www.gmw.com/electromagnets/Miniature/5201/5201.html
[26] A. A. Tulapurkar, Y. Suzuki, A. Fukushima, H. Kubota, H. Maehara, K. Tsunekawa, D. D. Djayaprawira, N. Watanabe, and S. Yuasa, Nature (London) **438**, 339 (2005).
[27] V. Tiberkevich and A. N. Slavin, Presentation DP-05 at the Intermag 2008 Conference, Madrid, May 2008 (unpublished).
[28] G. Finocchio, I. N. Krivorotov, L. Torres, R. A. Buhrman, D. C. Ralph, and B. Azzerboni, Phys. Rev. B **76**, 174408 (2007).
[29] J. C. Slonczewski, J. Magn. Magn. Mater. **247**, 324 (2002).